PROCEEDINGS OF SCIENCE

Applying the Worldvolume Hybrid Monte Carlo method to the two-dimensional Hubbard model[†]

Masafumi Fukuma[a] **and Yusuke Namekawa**[b,*]

[a] *Department of Physics, Kyoto University, Kyoto 606-8502, Japan*

[b] *Education and Research Center for Artificial Intelligence and Data Innovation, Hiroshima University, Hiroshima 739-8521, Japan*

E-mail: fukuma@gauge.scphys.kyoto-u.ac.jp, namekawa@hiroshima-u.ac.jp

The Worldvolume Hybrid Monte Carlo (WV-HMC) method [arXiv:2012.08468] is a low-cost algorithm that solves the sign problem without introducing the ergodicity problem. We apply the method to the Hubbard model on a two-dimensional spatial lattice, which can also be regarded as a prototype of QCD at finite density. We first explain the basic algorithms to treat fermion determinants in the WV-HMC method, and then show the computational cost scaling that varies depending on the choice of solver. We also compare the obtained results of observables with those using two other major numerical methods: the ALF (Algorithms for Lattice Fermions) and the Tensor Renormalization Group.

The 41st International Symposium on Lattice Field Theory (LATTICE2024)
28 July - 3 August 2024
Liverpool, UK

[†]Report No.: KUNS-3035
[*]Speaker

PoS(LATTICE2024)053

1. Introduction

Markov chain Monte Carlo (MCMC) method is a powerful tool for analyzing physical systems in a nonperturbative way. However, for systems with complex actions, the MCMC simulations often fail to provide accurate results due to the difficulty of numerically evaluating oscillatory integrals. Among various approaches to this *sign problem*, we focus on the Lefschetz thimble approach [1–3]. Although the original Lefschetz thimble method suffers from the ergodicity problem, the tempered Lefschetz thimble (TLT) method [4] succeeds in solving the sign problem without introducing the ergodicity problem. This method has been further developed into the Worldvolume Hybrid Monte Carlo (WV-HMC) method [5–7], which reduces simulation costs significantly.

The Hubbard model [8] is one of the simplest but nontrivial models describing strongly correlated electrons in a solid, and its Quantum Monte Carlo calculations based on the auxiliary field method suffer from the sign problem when systems are away from half filling. This model can also be regarded as a prototype of QCD at finite density. In this article, we apply the WV-HMC method to the two-dimensional Hubbard model. We first explain the basic algorithms to treat fermion determinants in the WV-HMC method, and then show the computational cost scaling that varies depending on the choice of solver. We also compare the obtained results of observables with those using two other major numerical methods: the ALF (Algorithms for Lattice Fermions) and the Tensor Renormalization Group. Our earlier study has been reported in Ref. [9].

2. WV-HMC method

We consider the expectation value of an observable $O(x)$ that is defined by the path integral

$$\langle O \rangle \equiv \frac{\int_{\mathbb{R}^N} dx\, e^{-S(x)}\, O(x)}{\int_{\mathbb{R}^N} dx\, e^{-S(x)}}, \tag{1}$$

where $\mathbb{R}^N = \{x\}$ is the configuration space of N degrees of freedom and $S(x) \in \mathbb{C}$ the complex action. Since $e^{-S(x)}$ is complex-valued, it cannot be regarded as a probability distribution and the MCMC is not applicable directly. The naïve reweighting method leads to highly oscillatory integrals and requires a huge number of configurations, $N_{\text{conf}} = e^{O(N)}$, in order for statistical errors to be relatively smaller than exponentially small mean values.

The Lefschetz thimble method [1–3] attempts to solve the sign problem by complexifying the dynamical variable $x \in \mathbb{R}^N$ to $z \in \mathbb{C}^N$ and deforming the integration surface $\mathbb{R}^N$ to the vicinity of Lefschetz thimbles where $\operatorname{Im} S(z)$ is constant. The deformation is made according to the anti-holomorphic flow:

$$\dot{z} = \overline{\partial S(z)}, \quad z|_{t=0} = x. \tag{2}$$

This flow sends the original integration surface $\Sigma_0 = \mathbb{R}^N$ to $\Sigma_t = \{z_t(x) \,|\, x \in \Sigma_0\}$. Thanks to Cauchy's theorem, the deformation does not change the integrals as long as $e^{-S(z)}$ and $e^{-S(z)}\, O(z)$ are entire functions over $\mathbb{C}^N$ (as is the case for most of interesting systems including the Hubbard model),

$$\langle O \rangle = \frac{\int_{\Sigma_t} dz\, e^{-S(z)}\, O(z)}{\int_{\Sigma_t} dz\, e^{-S(z)}}. \tag{3}$$

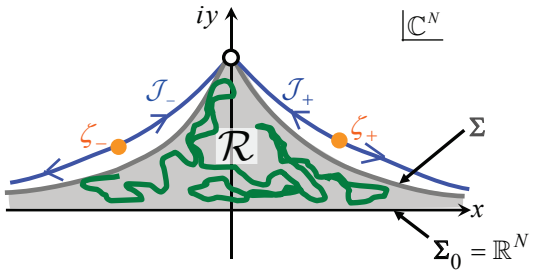

Figure 1: Worldvolume $\mathcal{R}$ (figure taken from Ref. [7]). In the figure, $\zeta_\pm$ are critical points, and $\mathcal{J}_\pm$ are the associated Lefschetz thimbles that are separated by a zero of $e^{-S(z)}$ (white circle). Configurations can move from one branch of Σ to another branch by passing through a detour in $\mathcal{R}$.

As flow time t increases, the deformed surface Σ_t approaches the vicinity of a set of Lefschetz thimbles, but some part will be attached to zeros of $e^{-S(z)}$ before Σ_t reaches the destination Σ, where the oscillatory behaviors are relaxed enough (see Fig. 1). Since these zeros separate Lefschetz thimbles, MCMC simulations on Σ will suffer from the ergodicity problem.

The WV-HMC algorithm [5] resolves this ergodicity problem by extending the configuration space from Σ to the worldvolume $\mathcal{R} \equiv \cup_t \Sigma_t = \{z_t(x) \,|\, t \in \mathbb{R},\, x \in \mathbb{R}^N\}$. The point is again Cauchy's theorem which guarantees that the numerator and the denominator in Eq. (3) do not depend on t, and we can average them over t with an arbitrary weight $e^{-W(t)}$. It leads to an integration over $\mathcal{R}$:

$$\langle O \rangle = \frac{\int dt\, e^{-W(t)} \int_{\Sigma_t} dz\, e^{-S(z)}\, O(z)}{\int dt\, e^{-W(t)} \int_{\Sigma_t} dz\, e^{-S(z)}} \equiv \frac{\langle \mathcal{F}(z)\, O(z) \rangle_{\mathcal{R}}}{\langle \mathcal{F}(z) \rangle_{\mathcal{R}}}. \tag{4}$$

Here, the reweighted average on $\mathcal{R}$ is defined as

$$\langle g(z) \rangle_{\mathcal{R}} \equiv \frac{\int_{\mathcal{R}} |dz|_{\mathcal{R}}\, e^{-V(z)}\, g(z)}{\int_{\mathcal{R}} |dz|_{\mathcal{R}}\, e^{-V(z)}} \tag{5}$$

with $|dz|_{\mathcal{R}}$ the invariant volume element of $\mathcal{R}$, $V(z) \equiv \mathrm{Re}\, S(z) + W(t(z))$ the potential, and $\mathcal{F}(z)$ is the reweighting factor,

$$\mathcal{F}(z) \equiv \frac{e^{-S(z)-W(t(z))}\, dt\, dz}{e^{-V(z)}\, |dz|_{\mathcal{R}}} = \frac{dt\, dz}{|dz|_{\mathcal{R}}} e^{-i\, \mathrm{Im}\, S(z)}. \tag{6}$$

We perform the Hybrid Monte Carlo simulation on the worldvolume $\mathcal{R}$ using the constrained molecular dynamics (RATTLE [3]) combined with a simplified Newton algorithm [7].

3. Hubbard model

The Hubbard model on a d-dimensional spatial lattice is defined by the following Hamiltonian (with a chemical potential term):

$$\begin{aligned} \hat{H}_\mu &= \hat{H} - \mu \hat{N} \\ &\equiv -\kappa \sum_{\mathbf{x},\mathbf{y}} \sum_{\sigma=\uparrow,\downarrow} J_{\mathbf{xy}}\, c^\dagger_{\mathbf{x},\sigma} c_{\mathbf{y},\sigma} + U \sum_{\mathbf{x}} n_{\mathbf{x},\uparrow} n_{\mathbf{x},\downarrow} - \mu \sum_{\mathbf{x}} (n_{\mathbf{x},\uparrow} + n_{\mathbf{x},\downarrow}). \end{aligned} \tag{7}$$

Here, $c_{\mathbf{x},\sigma}$ ($c^\dagger_{\mathbf{x},\sigma}$) is the annihilation (creation) operator of an electron of spin σ (=↑, ↓) at site $\mathbf{x} = (x_i)$, $J = (J_{\mathbf{xy}})$ is the adjacency matrix, where $J_{\mathbf{xy}}$ takes unity when $\mathbf{x}$ and $\mathbf{y}$ are nearest neighbors and takes zero otherwise, and $n_{\mathbf{x},\sigma} \equiv c^\dagger_{\mathbf{x},\sigma} c_{\mathbf{x},\sigma}$. Also, κ is the hopping parameter, U the on-site repulsion strength, and μ the chemical potential for the number operator $\hat{N} = \sum_{\mathbf{x}} \sum_\sigma n_{\mathbf{x},\sigma}$. We assume that the model is defined on a periodic, bipartite square lattice of linear size L_s (and thus the spatial volume is given by $V_d \equiv L_s^d$). In order to make manifest the real-valuedness of the bosonized action (to be introduced below) at half filling, we make the particle-hole transformation for the spin-down variable and write

$$a_{\mathbf{x}} \equiv c_{\mathbf{x}\uparrow}, \quad b_{\mathbf{x}} \equiv (-1)^{\mathbf{x}} c^\dagger_{\mathbf{x}\downarrow}, \tag{8}$$

where $(-1)^{\mathbf{x}} \equiv (-1)^{\sum_i x_i}$ is the parity of site $\mathbf{x}$. The Hamiltonian (7) then takes the following form up to an additive constant:

$$\hat{H}_\mu = -\kappa \sum_{\mathbf{x},\mathbf{y}} J_{\mathbf{xy}} \, (a^\dagger_{\mathbf{x}} a_{\mathbf{y}} + b^\dagger_{\mathbf{x}} b_{\mathbf{y}}) + \frac{U}{2} \sum_{\mathbf{x}} (n^a_{\mathbf{x}} - n^b_{\mathbf{x}})^2 - \tilde{\mu} \sum_{\mathbf{x}} (n^a_{\mathbf{x}} - n^b_{\mathbf{x}}), \tag{9}$$

where $n^a_{\mathbf{x}} \equiv a^\dagger_{\mathbf{x}} a_{\mathbf{x}}$, $n^b_{\mathbf{x}} \equiv b^\dagger_{\mathbf{x}} b_{\mathbf{x}}$, and $\tilde{\mu} \equiv \mu - U/2$. The point $\mu = U/2$ (equivalently, $\tilde{\mu} = 0$) corresponds to the half filling $\langle n_{\mathbf{x},\uparrow} + n_{\mathbf{x},\downarrow} \rangle = 1$ (i.e., $\langle n^a_{\mathbf{x}} - n^b_{\mathbf{x}} \rangle = 0$). We also introduce a redundant parameter α ($0 \le \alpha \le 1$) [10],

$$(n^a_{\mathbf{x}} - n^b_{\mathbf{x}})^2 = \alpha (n^a_{\mathbf{x}} - n^b_{\mathbf{x}})^2 - (1-\alpha)(n^a_{\mathbf{x}} + n^b_{\mathbf{x}} - 1)^2 + (1-\alpha). \tag{10}$$

Although the choice of α does not change the expectation values of observables, it affects the extent of the sign and the ergodicity problems [10–12]. If $\alpha = 0$, the sign problem is mild but we encounter a severe ergodicity problem. As the value of α increases, the ergodicity problem gets milder but severer sign problem will arise instead.

The grand canonical partition function on the lattice is defined by

$$Z \equiv \mathrm{tr}\, e^{-\beta \hat{H}_\mu}. \tag{11}$$

Introducing a Hubbard-Stratonovich field for each of $(n^a_{\mathbf{x}} - n^b_{\mathbf{x}})^2$ and $(n^a_{\mathbf{x}} + n^b_{\mathbf{x}} - 1)^2$ (denoted by A and B, respectively), we have

$$Z = \int dA\, dB\, e^{-S(A,B)} = \int dA\, dB\, e^{-S_0(A,B)} \, \det D_a(A,B) \, \det D_b(A,B). \tag{12}$$

Here, $S_0(A,B) \equiv (1/2) \sum_x (A_x^2 + B_x^2)$ with coordinates $x = (\ell, \mathbf{x})$, and the fermion operators are defined by

$$D_{a/b}(A,B) \equiv e^{\pm(\epsilon\tilde{\mu} + i c_0) A + c_1 B - c_1^2} - (1 - \epsilon\kappa J)\, \Lambda_0^{-1} + O(\epsilon^2), \tag{13}$$

$$(\Lambda_0)_{xy} = \begin{cases} \delta_{\ell+1,m}\, \delta_{\mathbf{xy}} & (0 \le \ell < N_t - 1) \\ -\delta_{0,m}\, \delta_{\mathbf{xy}} & (\ell = N_t - 1)\,, \end{cases} \tag{14}$$

with $c_0 \equiv \sqrt{\alpha\epsilon U}$, $c_1 \equiv \sqrt{(1-\alpha)\epsilon U}$. There can be two ways to deal with the fermion determinants $\det D_{a/b}(A,B)$. One is to use (A,B) as the only dynamical variables and consider the action

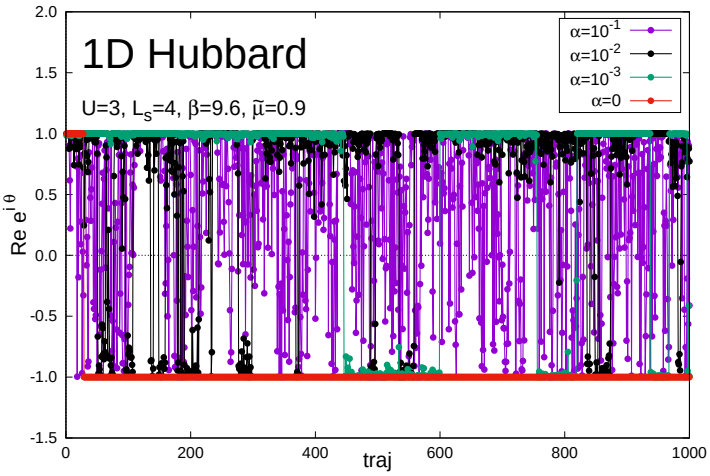

Figure 2: Trajectory dependence of the phase factor for various α.

$S(A,B) = S_0(A,B) - \mathrm{tr}\ln\det D_a(A,B) - \mathrm{tr}\ln\det D_b(A,B)$. In this case, the numerical cost to generate a configuration will be $O(N^3)$. The other is to introduce real pseudofermions for $M_{a/b} \equiv D_{a/b}D_{a/b}^T$ and use iterative solvers to invert $M_{a/b}$. The latter is justified only when $\mathrm{Re}\,(M_{a/b}^{-1}) > 0$, but the numerical cost will be reduced to $O(N^2)$ by using CG-type solvers. As a physical observable, we use the number density

$$n(A,B) \equiv -\frac{1}{V_d}\frac{\partial S(A,B)}{\partial \mu} + 1, \tag{15}$$

which agrees with $\hat{N}/V_d$ up to $O(\epsilon^2)$.

4. Result for $1D$ Hubbard model

We first consider the one-dimensional Hubbard model to demonstrate that α certainly affects the extent of the sign and the ergodicity problems. We set the hopping parameter $\kappa = 1$, the repulsion strength $U = 3$, the inverse temperature $\beta = (N_t\epsilon) = 9.6$ with $\epsilon = 0.32$, and the spatial size $L_s = 4$. Since the sign problem is mild in this setup, we perform simulations using the naïve reweighting method. Figure 2 represents typical histories of the phase factor for various values of α. The result for $\alpha = 0$ suffers from long autocorrelation, indicating the existence of severe ergodicity problem. As α increases, the value of the phase factor changes more frequently, from which we expect that the ergodicity problem is getting relaxed. In fact, we see from Fig. 3 that, although the simulation with $\alpha = 0$ fails to reproduce the exact values of number density around $\tilde{\mu} = 1$, the simulation with $\alpha = 10^{-2}$ succeeds in reproducing the exact values. Based on this result, we set α to the minimum among the values with which the phase factor frequently changes in the following analysis.

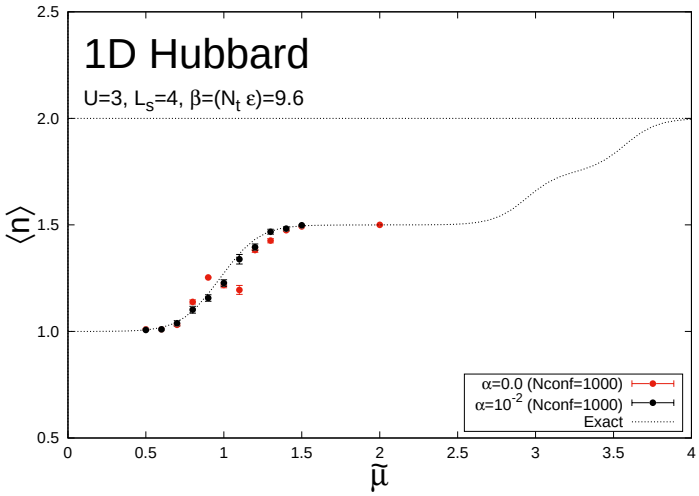

Figure 3: The number density for $\alpha = 0$ and 10^{-2}.

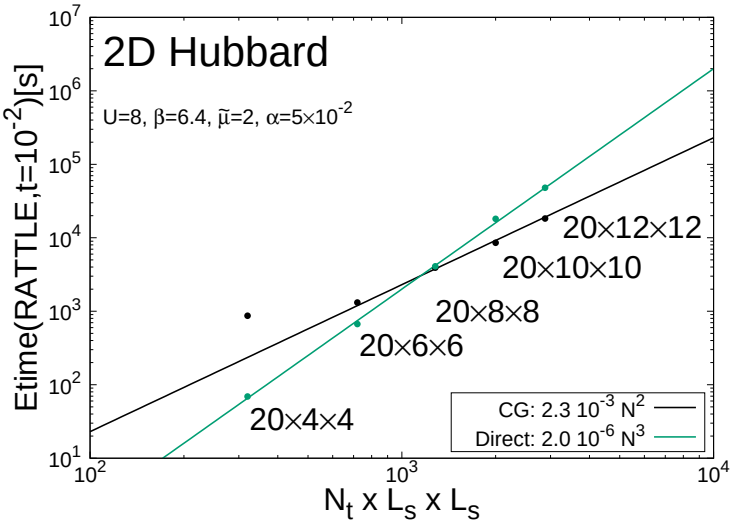

Figure 4: Elapsed time of each RATTLE step using direct or CG-type solvers for $D_{a/b}$.

5. Result for $2D$ Hubbard model

We first investigate the computational cost scaling for various spatial volumes with fixed $\beta\,(=6.4)$ and fixed flow time $t\,(=10^{-2})$. Figure 4 shows the elapsed time of each RATTLE step when we use direct or iterative (CG-type) solvers for $D_{a/b}$. The expected computational cost scaling is observed: $O(N^3)$ for direct solvers and $O(N^2)$ for CG-type solvers.

We then perform the WV-HMC simulation for 2D Hubbard model with spatial lattice size $L_s \times L_s = 6 \times 6$. We adopt direct solvers, setting the hopping parameter $\kappa = 1$, the repulsion strength $U = 8$, and the inverse temperature $\beta = (N_t\epsilon) = 6.4$ with $N_t = 20$ and $\epsilon = 0.32$. The lower and upper values of the flow time are set to $T_0 = 0$ and $T_1 = 0.1$, respectively. We compare the results obtained by WV-HMC with those by two non-thimble methods. One is ALF (Algorithms for Lattice

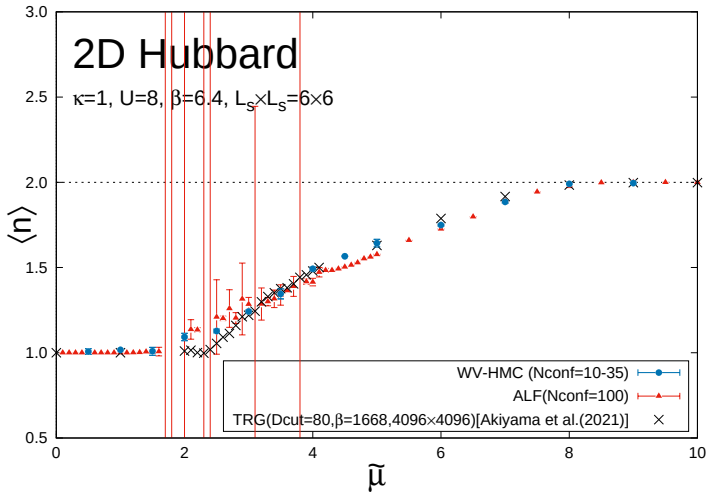

Figure 5: The number density obtained with three methods: WV-HMC, ALF [13, 14], and TRG [15].

Fermions) [13, 14], which is a well-established algorithm developed in condensed matter physics. It is robust and fast when the system is free from the sign problem, but needs an exponentially large computational time when the sign problem is severe. We use the same model parameters as the WV-HMC simulation except that we set $N_t = 80$ and $\epsilon = 0.08$ for ALF. The other non-thimble method is the TRG method [15], where the bond dimension is set to 80 and the number of TRG iterations is chosen such that the corresponding lattice size is $L_s \times L_s = 4096 \times 4096$ and $N_t = 2^{24}$ ($\beta = 1688$), which is much larger than that of the WV-HMC and the ALF.

Figure 5 represents the results for the number density. In the region $\tilde{\mu} \lesssim 1.5$ or $\tilde{\mu} \gtrsim 4.0$, where the sign problem is relatively mild, three of the algorithms (WV-HMC, ALF and TRG) give the same results within statistical errors. On the other hand, in the region of severe sign problem, $1.5 \lesssim \tilde{\mu} \lesssim 4.0$, the ALF results exhibit huge statistical errors due to the sign problem, while the WV-HMC results succeed in keeping statistical errors to small values because of the good control of WV-HMC over the sign problem. WV-HMC and TRG give similar values in most of the region, but the results do not agree for $2.0 \lesssim \tilde{\mu} \lesssim 2.5$. Although the sample size is not yet large enough to make a definite statement, we expect that the discrepancy is due to the smallness of the lattice size. This will become clear as we increase the lattice size and the sample size for WV-HMC (as we are investigating now).

6. Conclusion

We have applied the WV-HMC method [5–7] to the two-dimensional Hubbard model. We confirmed that the computational cost scales as $O(N^3)$ for direct solvers and as $O(N^2)$ for CG-type solvers with pseudofermions, as we expected. We also checked that the number density obtained with WV-HMC agrees with the results of ALF and TRG in the region of mild sign problem. Furthermore, we demonstrate that WV-HMC keeps statistical errors to small values even in the region of severe sign problem where ALF loses control over statistical errors.

We are now enlarging the temporal and the spatial sizes for WV-HMC simulations in order to make more precise comparison with other methods and eventually to investigate the phase structure of the Hubbard model. We are also applying the WV-HMC to other systems, such as gauge theories with θ-term (see Ref. [16]), finite-density QCD, and real-time dynamics of quantum many-body systems.

Acknowledgments

The authors thank Sinya Aoki, Fakher F. Assaad, Masatoshi Imada, Ken-Ichi Ishikawa, Issaku Kanamori, Yoshio Kikukawa, Nobuyuki Matsumoto, and Maksim Ulybyshev for valuable discussions. This work was partially supported by JSPS KAKENHI Grant Numbers JP20H01900, JP21K03553, JP23H00112, JP23H04506, JP24K07052 and by MEXT as "Program for Promoting Researches on the Supercomputer Fugaku" (Simulation for basic science: approaching the new quantum era, JPMXP1020230411) and used computational resources of the supercomputer Fugaku provided by the RIKEN Center for Computational Science (Project ID: hp230207, hp240213).

References

[1] E. Witten, *Analytic Continuation Of Chern-Simons Theory*, *AMS/IP Stud. Adv. Math.* **50** (2011) 347 [1001.2933].

[2] AuroraScience collaboration, *New approach to the sign problem in quantum field theories: High density QCD on a Lefschetz thimble*, *Phys. Rev. D* **86** (2012) 074506 [1205.3996].

[3] H. Fujii, D. Honda, M. Kato, Y. Kikukawa, S. Komatsu and T. Sano, *Hybrid Monte Carlo on Lefschetz thimbles - A study of the residual sign problem*, *JHEP* **10** (2013) 147 [1309.4371].

[4] M. Fukuma and N. Umeda, *Parallel tempering algorithm for integration over Lefschetz thimbles*, *PTEP* **2017** (2017) 073B01 [1703.00861].

[5] M. Fukuma and N. Matsumoto, *Worldvolume approach to the tempered Lefschetz thimble method*, *PTEP* **2021** (2021) 023B08 [2012.08468].

[6] M. Fukuma, N. Matsumoto and Y. Namekawa, *Statistical analysis method for the worldvolume hybrid Monte Carlo algorithm*, *PTEP* **2021** (2021) 123B02 [2107.06858].

[7] M. Fukuma, *Simplified Algorithm for the Worldvolume HMC and the Generalized Thimble HMC*, *PTEP* **2024** (2024) 053B02 [2311.10663].

[8] J. Hubbard, *Electron correlations in narrow energy bands*, *Proc. Roy. Soc. A* **276** (1963) 238.

[9] M. Fukuma and Y. Namekawa, *Applying the Worldvolume Hybrid Monte Carlo method to the finite-density complex ϕ^4 model and the Hubbard model*, *PoS* **LATTICE2023** (2024) 178.

[10] S. Beyl, F. Goth and F.F. Assaad, *Revisiting the Hybrid Quantum Monte Carlo Method for Hubbard and Electron-Phonon Models*, *Phys. Rev. B* **97** (2018) 085144 [1708.03661].

[11] M.V. Ulybyshev and S.N. Valgushev, *Path integral representation for the Hubbard model with reduced number of Lefschetz thimbles*, 1712.02188.

[12] J.-L. Wynen, E. Berkowitz, C. Körber, T.A. Lähde and T. Luu, *Avoiding Ergodicity Problems in Lattice Discretizations of the Hubbard Model*, *Phys. Rev. B* **100** (2019) 075141 [1812.09268].

[13] M. Bercx, F. Goth, J.S. Hofmann and F.F. Assaad, *The ALF (Algorithms for Lattice Fermions) project release 1.0. Documentation for the auxiliary field quantum Monte Carlo code*, *SciPost Phys.* **3** (2017) 013 [1704.00131].

[14] ALF collaboration, *The ALF (Algorithms for Lattice Fermions) project release 2.4. Documentation for the auxiliary-field quantum Monte Carlo code*, *SciPost Phys. Codeb.* **2022** (2022) 1 [2012.11914].

[15] S. Akiyama, Y. Kuramashi and T. Yamashita, *Metal–insulator transition in the (2+1)-dimensional Hubbard model with the tensor renormalization group*, *PTEP* **2022** (2022) 023I01 [2109.14149].

[16] M. Fukuma, *Worldvolume Hybrid Monte Carlo algorithm for group manifolds*, *in preparation* .